

Article

Characterization of Lignin Structures in *Phyllostachys edulis* (Moso Bamboo) at Different Ages

Yikui Zhu ^{1,2}, Jiawei Huang ^{1,2}, Kaili Wang ^{1,2}, Bo Wang ³ , Shaolong Sun ⁴, Xinchun Lin ⁵, Lili Song ⁵, Aimin Wu ^{1,2,*} and Huiling Li ^{1,2,*}

¹ State Key Laboratory for Conservation and Utilization of Subtropical Agro-Bioresources, South China Agricultural University, Guangzhou 510642, China; ZhuYKWerid@163.com (Y.Z.); jiawehuangkawy@gmail.com (J.H.); wangkl_china@163.com (K.W.)

² Guangdong Key Laboratory for Innovative Development and Utilization of Forest Plant Germplasm, College of Forestry and Landscape Architectures, South China Agricultural University, Guangzhou 510642, China

³ The Key Laboratory of Plant Molecular Breeding of Guangdong Province, College of Agriculture, South China Agricultural University, Guangzhou 510642, China; bowang@scau.edu.cn

⁴ College of Natural Resources and Environment, South China Agricultural University, Guangzhou 510642, China; sunshaolong328@scau.edu.cn

⁵ State Key Laboratory of Subtropical Silviculture, Zhejiang A&F University, Lin'an 311300, China; lxc@zafu.edu.cn (X.L.); lilisong@zafu.edu.cn (L.S.)

* Correspondence: wuaimin@scau.edu.cn (A.W.); lihl@scau.edu.cn (H.L.)

Received: 13 December 2019; Accepted: 7 January 2020; Published: 10 January 2020



Abstract: Bamboo is a gramineous plant widely distributed in China and has great prospects. Normally, local people cut bamboo culm at first year for paper milling or at six years for construction. Understanding lignin changes in bamboo with aging is necessary for better exploring the application of bamboo at different ages and can also promote the application of bamboo more effectively. Based on the previous study, the chemical structure and the lignin content of bamboo at different ages were further explored by FT-IR, GPC, NMR and other chemical methods in this paper. Results showed that the lignin structures of bamboo at different ages were similar with three monomers of S, G and H, but the molecular weight increased with age. Quantitative structure estimation further confirmed that S-type lignin content and S/G ratio of bamboo lignin constantly increased with age.

Keywords: *Phyllostachys edulis*; lignin structures; molecular weight; S:G ratio; NMR

1. Introduction

Bamboo belong to the Gramineae plant group, which is widely distributed in Asian countries [1]. Due to the global shortage of forest resources, bamboo is considered the best plant species to replace wood because of its rapid growth, high tensile strength, good toughness and ductility [2]. More attention has focused on the broad prospects of bamboo as an energy plant besides the traditional pulp industry in recent years, such as packaging industry [3,4]. The application of bamboo is mainly related to its secondary cell wall [5]. Compared with the secondary cell wall of wood, bamboo has a more obviously layered structure. Unlike wood, the material properties of bamboo will not be affected by its high-speed growth. Moreover, characteristics of bamboo such as high mechanical strength, good toughness and ductility has attracted growing attention from scholars [6]. However, there are few studies on the changes of bamboo cell wall in the process of lignification with age, which restricts the application of bamboo as an energy plant to some extent. The main components of the secondary cell wall of *Phyllostachys pubescens* (bamboo) are cellulose, hemicellulose and lignin. The lignification of bamboo is a dynamic process of deposition of lignin in the secondary cell wall [7].

Therefore, understanding the changes of lignin can give an insight into the cell wall changes during bamboo lignification.

Lignin is an amorphous polymer which contains three different cinnamyl alcohol monomers: coniferyl, sinapyl, and *p*-coumaryl alcohols, each of which leads to a corresponding type of lignin unit named guaiacyl, syringyl, and *p*-hydroxyphenyl, respectively, linked by C–C bonds and ether bonds [8]. As the second most abundant natural polymer, lignin accounts for about 30% of the organic carbon in the biosphere, and it is composed of aromatic monomers [9]. In the process of plant growth, lignin is polymerized *in vivo* via an enzyme-mediated dehydrogenation polymerization (lignification), resulting in a cross-linked amorphous material with both C–C and ether bonds [10]. Moreover, lignin plays an important role in strengthening cell-to-cell connections, increasing cell wall strength and resisting pathogens during subsequent growth [11]. In the field of biological research, modern biotechnology provides precise manipulation techniques for the biosynthesis of lignin, which can alter the lignin structure in plants by up- or down-regulating specific genes. Therefore, future research on lignin should combine the synergy between biology and chemistry. Nowadays, lignin is widely used in the production of aromatic chemical products instead of petroleum-based raw materials. The main trends are the separation of three main aromatic monomers by depolymerization of lignin: benzene, toluene, and xylene, then subsequent synthesis of other chemical products [9,12,13].

Although the application prospect of lignin is very clear, it now has more obstacles to its efficient utilization. The extraction methods of lignin can be divided into two categories: (1) use of a neutral solvent to dissolve and extract a portion of the lignin while retaining the carbohydrates; (2) an enzymatic hydrolysis method to degrade the carbohydrates to retain the residual lignin [9]. Although lignin separation methods have been studied for many years, there are still many scholars working on new techniques to explore new lignin separation approaches with higher yields and less structural damage [14]. Monomers extracted from lignin are not suitable for direct preparation of compounds [9]. The physical and chemical properties of lignin produced by content changes of nonpolymeric alcohols in different plant sources are quite different, which is one of the obstacles in industrialization. In the process of plant lignification, the formation of lignin monomer from cross-linking to each other to form lignin macromolecules adds further complexity to the lignin structure [15]. Therefore, the structural complexity of lignin of different species is also an important constraint.

Bamboo, which is one of the rapid growth lignocellulosic biomass species, is considered to be a suitable raw material for the lignin industry due to its characteristics of wide distribution and high lignin content [16]. Large-scale plantings of bamboo usually takes no more than six years to reach harvestable size in China. The study of the lignification of bamboo has mostly focused on the growth pattern and anatomical structure of bamboo [17]. However, the chemical quantification of lignin has not been explored at different bamboo ages. In general, bamboo with lower lignin content is favorable for the paper making and bioenergy industry applications, while bamboo with higher lignin content is more suitable for use in the building and furniture industries. Therefore, a clear understanding of the changes in bamboo lignin with age can further guide the follow-up bamboo industry. The purpose of this paper is to investigate the changes in chemical structure and content of lignin of bamboo with ages (1–6 years old). Based on the previous research [17,18], the analysis of bamboo lignin in different years was carried out by Nuclear Magnetic Resonance (NMR), Fourier Transform infrared spectroscopy (FT-IR), Gel Permeation Chromatography (GPC), and changes in lignin chemical structures during the whole lignification process was observed visually.

2. Materials and Methods

2.1. Materials

1–6 year old bamboo used in this study were collected from Hangzhou, Zhejiang Province, China. Prior to the experiments, the bamboo was decorticated, then sieved to about 40-mesh size. The obtained particles were oven-dried at 55 °C to a constant weight. The composition analysis

(cellulose, hemicellulose and lignin) of bamboo was performed according to the procedure established by National Renewable Energy Laboratory [19].

2.2. Milled Wood Lignin (MWL) Isolation and Purification

The lignin of 1–6 year(s) old bamboo were isolated according to the previous literature [20]. First, 20 g of bamboo samples from different years after extraction and drying were subjected to ball milling for 2.5 h by a planetary ball mill (DECO-PBM-V, Deco Co., Ltd., Changsha, Hunan, China) at 300 rpm using zirconia balls of approximately 1 cm in diameter. After ball milling, the solid is re-baked for use. The dried solid was mixed with 96% dioxane (*w/v*, 1:20) and stirred for 2.5 h at 100 °C. After the reaction, the solid–liquid separation was carried out using a sand core funnel. The separated liquid was concentrated by a rotary evaporator (Rotavapor® R-300, BUCHI, Flawil, Switzerland), and then dropped into 3 volumes of 95% ethanol for 24 h to remove excess hemicellulose. After the reaction, centrifugation was carried out, and the liquid fraction was concentrated again. The concentrated liquid was dropped into 10 volumes of acid water (pH = 2, hydrochloric acid) to precipitate the desired lignin. The precipitated solid was freeze-dried to obtain the required lignin products.

2.3. Determination and Structural Characterization of Bamboo Lignin

FT-IR spectra of the prepared 1–6 year(s) old bamboo lignin samples were recorded on a spectrophotometer (Tensor 27, Bruker Optics, Karlsruhe, Germany) in the range of 1800–800 cm^{-1} using a KBr disc containing finely ground samples (1%) [21]. Lignin acetylation was carried out with reference to relevant literature [22], and the molecular weight of acetylated lignin was determined by GPC. In short, 1 mg acetylated lignin was dissolved in 1 mL of tetrahydrofuran ($\geq 99.0\%$, HPLC, Sigma, Oliver Township, MI, American), and then filtered through an organic phase filter and measured by GPC (Nexera UHPLC/HPLC System Shimadzu, Kyoto, Japan) [21]. Experiments were repeated three times to obtain the average values. NMR spectra (^{13}C NMR and 2D-HSQC spectra) of the lignin samples were obtained on a 600 MHz Bruker Avance (Tensor 27, Bruker Optics, Karlsruhe, Germany). The ^{13}C NMR analysis conditions were: 100 mg lignin dissolved in 0.5 mL DMSO- d_6 , sampling time was 1.35 s, relaxation time was 1.5 s, scanned 3000 times; 2D-HSQC analysis conditions were: 60 mg lignin dissolved in 0.5 mL DMSO- D_6 , the sampling time was 0.17 s, the relaxation time was 1.5 s, sampled 128 times, and the scanning time was 6 h [23].

3. Results and Discussion

3.1. Composition Analysis of 1–6 Year(s) Old Bamboo

The changes in contents of cellulose, hemicellulose and lignin were examined during the lignification of bamboo. Compared with hemicellulose, the contents of lignin and cellulose varied more obviously with ages (Figure 1). The lignification of bamboo is the generation of lignin. Our study showed that a growing trend (26–36%) of lignin content could be observed from 1–6 years old bamboo. However, the relative content of cellulose decreased (55–45%) with stable hemicellulose amount. The earliest phase of the growth of bamboo (between one and two years) is the rapid accumulation of biomass. After this, the stem grows rapidly to the maximum height, followed by the increase in strength and accumulation of dry mass. The processes of lignification and cell wall thickening begin after three years [24]. It can be seen from Figure 1 that the relative content of lignin in one and two-year old bamboo is almost the same, and the lignin contents of bamboo in three to six years old are significantly higher than those in the former. This phenomenon is consistent with the results about the chemical composition of bamboo during the lignification process [25]. The above results indicate that the growth rates of lignin, hemicellulose and cellulose are in the following order: lignin > hemicellulose > cellulose.

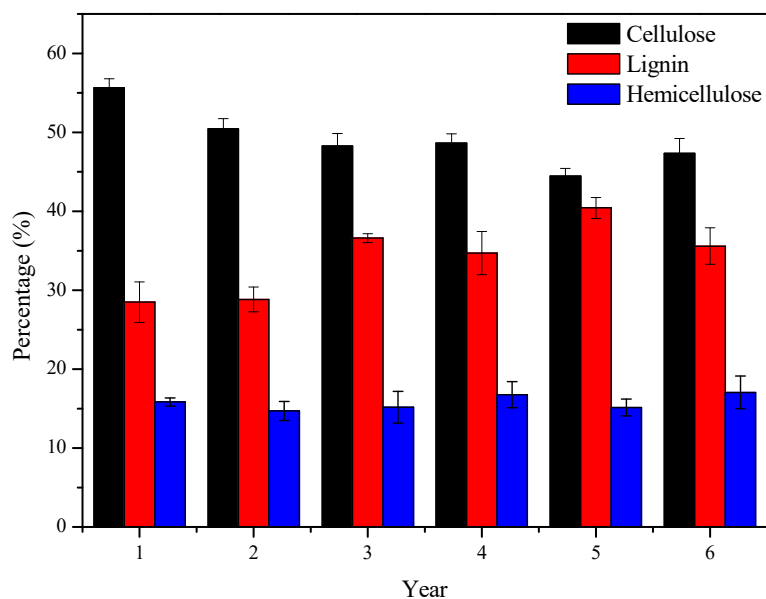


Figure 1. 1–6 years old bamboo composition analysis.

3.2. FT-IR Spectra

In order to investigate the changes of lignin structure during bamboo lignification, FT-IR was conducted to analyze the structure of lignin extracted from different annual bamboo, and the results are shown in Figure 2. Characteristic brands of lignin skeleton and fractions were assigned according to data from the literature. The absorbance at 1703 cm^{-1} corresponds to the conjugated carbonyl (C=O) [26]. Brands at 1600 cm^{-1} , 1501 cm^{-1} , and 1425 cm^{-1} are the characteristic peaks of the benzene ring structure, which proved that the bamboo lignin has a typical benzene ring structure [27]. The absorption peak at 1459 cm^{-1} is the C–H deformation vibration associated with the benzene ring [28]. The three absorption peaks are the characteristic peaks of lignin skeleton structure, their strengths are almost the same in each year, which proves that the lignin skeleton does not change significantly during the lignification of the bamboo. The peak at 1330 cm^{-1} is the absorption peak of the syringyl group and the condensed guaiacyl group. The absorption peak at 1265 cm^{-1} corresponds to the C=O stretching vibration in the guaiacyl ring, while the peak at 1228 cm^{-1} corresponds to the vibration of lignin C–C, C–O, C=O. The peak at 1167 cm^{-1} is attributed to the ester bond, which indicated that the bamboo lignin monomers are linked by ester bonds [29]. Peaks at 834 cm^{-1} , 1121 cm^{-1} and 1167 cm^{-1} were attributed to the three monomers of lignin, respectively, suggesting that the bamboo lignin contained three lignin monomers of S, G and H. FT-IR results indicate that the basic skeleton of lignin remains consistent in the process of bamboo lignification. Three lignin monomers of S, G and H exist in all bamboo lignin samples. FT-IR spectra of 1–6 years old bamboo lignin samples behave such that the absorption peak position and relative intensities are basically the same, which proves that the structure of bamboo lignin in different years had no major modifications occurred during lignification. Therefore, in order to better explore these changes, more analysis is necessary.

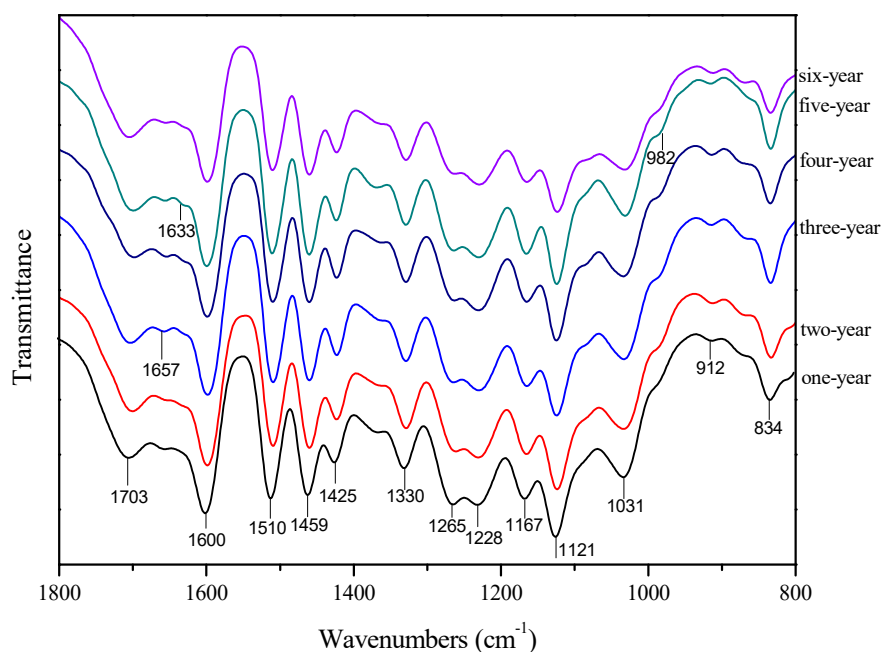


Figure 2. FT-IR spectra of 1–6 years old bamboo lignin.

3.3. Molecular Weight Analysis

Molecular weight is one of the important properties of polymers. The weight average (M_w) and number average (M_n) molecular weight of lignin obtained from one to six years-old bamboo were determined by GPC (Table 1). The M_w of 1–6 years-old bamboo lignin increased from 4586 to 5823 with age. Moreover, the molecular weight polydispersity coefficient PD (M_w/M_n) of lignin increased with the degree of lignification, which indicates that the molecular weight distribution of the obtained samples is wider. The change in molecular weight during lignification deepened, further indicating that the older the bamboo, the more suitable it is for the preparation of lignin-based composites than the lower-grade bamboo [30].

Table 1. Weight-average (M_w) and number-average (M_n) molecular weights and polydispersity (M_w/M_n) of 1–6 years old bamboo lignin samples.

| Age (Years) | M_w (g/mol) | M_n (g/mol) | M_w/M_n |
|-------------|---------------|---------------|-----------|
| 1 | 4586 | 2327 | 1.97 |
| 2 | 4954 | 2329 | 2.12 |
| 3 | 5245 | 2477 | 2.12 |
| 4 | 5410 | 2570 | 2.11 |
| 5 | 5670 | 2584 | 2.19 |
| 6 | 5823 | 2484 | 2.34 |

3.4. ^{13}C NMR Spectra

To further characterize the lignin structures with ages, different annual bamboo lignin were measured by ^{13}C NMR (Figure 3). Peak assignments are made by comparison with the data reported in the literature [31,32]. Overall, the lignin peaks of bamboo in different years are roughly the same in addition to peak intensity, which is consistent with the results of FT-IR. The characteristic peaks for coumarin esters appear at δ 166.5 ppm, δ 159.9 ppm, δ 144.3 ppm, δ 130.2 ppm, δ 125.1 ppm, δ 115.9 ppm, and δ 114.8 ppm, corresponding to C9, C4, C7, C2/6, C1, C3/5 and C8. The signal peaks of the C8 junction appeared in the six-year old bamboo lignin, indicating that the synthesis of lignin side chains occurred in the γ position during the lignification of bamboo. Characteristic signal peaks of S-type lignin unit appear at δ 152.3 ppm, δ 147.6 ppm, δ 138.2 ppm, δ 134.5 ppm, and δ 106.9 ppm, respectively,

corresponding to etherified C3/C5, non-etherified C3/C5, etherified C4, etherified C1, non-etherified C2/C6 connection location. The characteristic peaks of the G-type lignin unit appear at δ 145.1 ppm, δ 119.5 ppm, and δ 111.2 ppm, corresponding to non-etherified C4, C6 (etherified and non-etherified), and C2 (etherified and non-etherified) position. Peaks of H-type lignin unit appear at δ 130.2 ppm, which corresponds to the C2/C6 linkage. Both of the above signal peaks can be found in all bamboo lignin carbon spectra, which proves that the bamboo lignin is composed of three lignin monomers (S, G, and H). This phenomenon is consistent with the FT-IR results mentioned before. The results of ^{13}C NMR confirmed that the structure of lignin monomer and the substitution joint position did not change much during the lignification of bamboo.

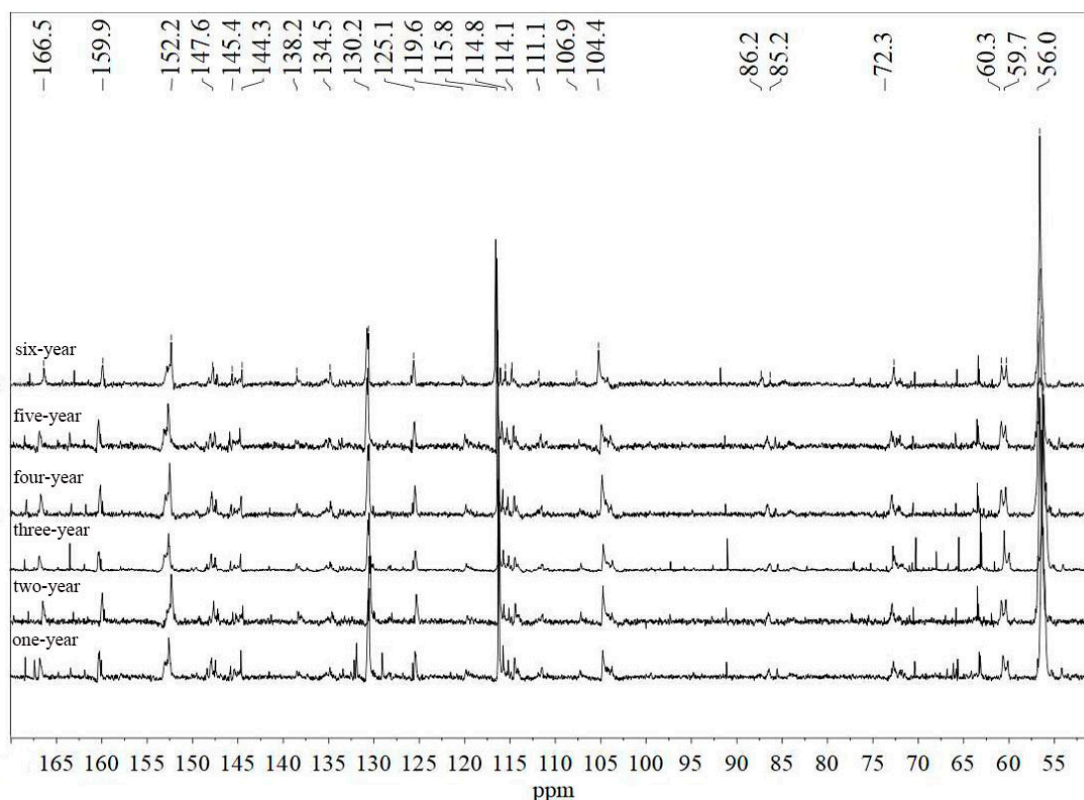


Figure 3. ^{13}C NMR spectra of 1–6 year-old bamboo lignins.

3.5. 2D-HSQC NMR Spectra

To better characterize lignin structure, 1–6 year-old bamboo lignin samples were further examined by 2D-HSQC spectra, which can indicate the side chain region ($\delta\text{C}/\delta\text{H}$ 50–90/2.5–6.0) and the aromatic ring region ($\delta\text{C}/\delta\text{H}$ 90–160/6.0–8.0). The main structure and signal attribution are compared with the reported data [8,33]. Results are shown in Figure 4 and Table 2.

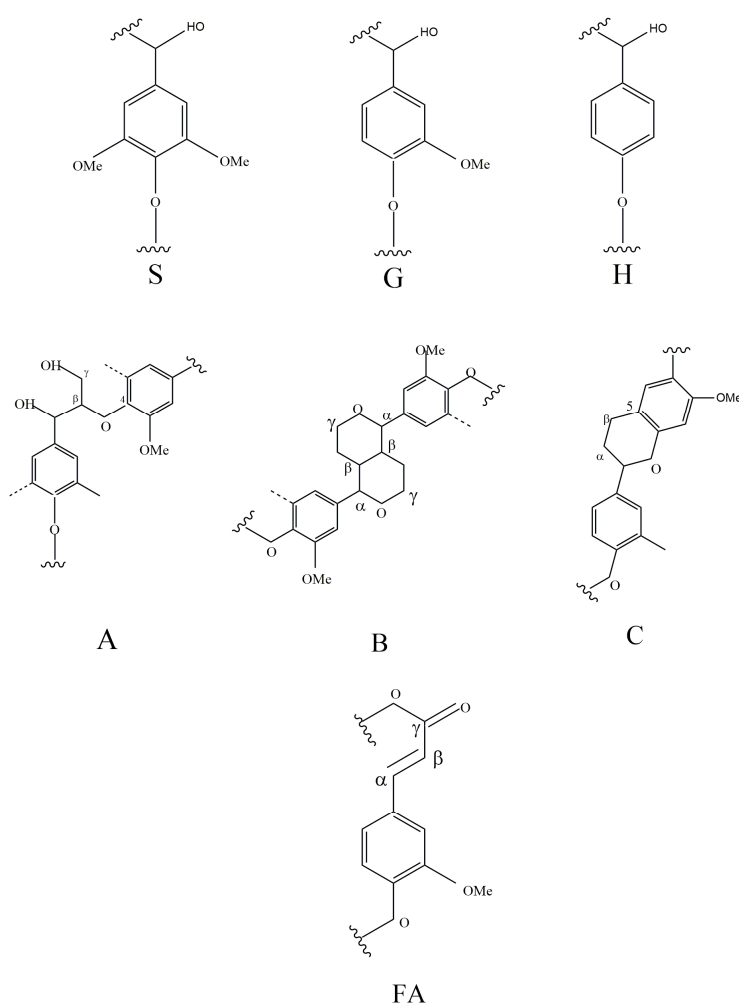


Figure 4. Main classical structures in the lignin preparations: (A) β -O-4 ether linkages; (B) resinol structures formed by β - β' / α -O- γ' / γ -O- α' linkages; (C) phenylcoumarane structures formed by β -5'/ α -O-4' linkages; (FA) Ferulates guaiacyl unit; (S) syringyl unit; (H) p-hydroxyphenyl units (G) guaiacyl units.

Table 2. Assignments of ^{13}C - ^1H cross signals in the HSQC spectra of the lignin.

| Label | $\delta\text{C}/\delta\text{H}$ (ppm) | $\delta\text{C}/\delta\text{H}$ (ppm) | Assignments |
|------------------|---------------------------------------|---------------------------------------|--|
| B' $_{\beta}$ | 49.8/2.56 | ND | C $_{\beta}$ -H $_{\beta}$ in β - β tetrahydrofuran (B') |
| C $_{\beta}$ | 53.1/3.46 | ND | C $_{\beta}$ -H $_{\beta}$ in phenylcoumaran (C) |
| B $_{\beta}$ | 53.5/3.07 | 53.5/3.07 | C $_{\beta}$ -H $_{\beta}$ in β - β (resinol) (B) |
| D $_{\beta}$ | 59.8/2.75 | ND | C $_{\beta}$ -H $_{\beta}$ in spirodienones (D) |
| OCH $_3$ | 56.4/3.70 | 55.6/3.76 | C-H in methoxyls |
| A $_{\gamma}$ | 59.9/3.35 | 62.0/4.08 | C $_{\gamma}$ -H $_{\gamma}$ in β -O-4 substructures (A) |
| A' $_{\gamma}$ | 63.0/4.36 | 63.0/3.8 | C $_{\gamma}$ -H $_{\gamma}$ in γ -acylated β -O-4 (A') |
| C $_{\gamma}$ | 62.2/3.76 | 64.3/4.33 | C $_{\gamma}$ -H $_{\gamma}$ in phenylcoumaran (C) |
| I $_{\gamma}$ | 61.2/4.09 | 64.1/4.66 | C $_{\gamma}$ -H $_{\gamma}$ in cinnamyl alcohol end-groups (I) |
| I' $_{\gamma}$ | 64.0/4.80 | 64.2/4.82 | C $_{\gamma}$ -H $_{\gamma}$ in acylated cinnamyl alcohol (I') |
| B $_{\gamma}$ | 71.2/3.82 | 71.7/3.84 | C $_{\gamma}$ -H $_{\gamma}$ in β - β resinol (B) |
| A $_{\alpha}$ | 71.8/4.86 | 73.8/5.93 | C $_{\alpha}$ -H $_{\alpha}$ in β -O-4 unit (A) (<i>Erythro</i>) |
| A $_{\alpha}$ | 71.8/4.86 | 73.8/5.93 | C $_{\alpha}$ -H $_{\alpha}$ in β -O-4 unit (A) (<i>Thero</i>) |
| A $_{\beta}$ (G) | 83.4/4.38 | 76.6/5.07 | C $_{\alpha}$ -H $_{\alpha}$ in β -O-4 linked to G(A) |
| B $_{\alpha}$ | 84.8/4.66 | 85.6/4.70 | C $_{\alpha}$ -H $_{\alpha}$ in β - β resinol (B) |
| B' $_{\alpha}$ | 83.2/4.94 | ND | C $_{\alpha}$ -H $_{\alpha}$ in β - β (B', tetrahydrofuran) |

Table 2. Cont.

| Label | $\delta C/\delta H$ (ppm) | $\delta C/\delta H$ (ppm) | Assignments |
|-------------------|---------------------------|---------------------------|---|
| A'' $_{\beta}$ | 82.8/5.23 | ND | C $_{\beta}$ -H $_{\beta}$ in β -O-4 substructures (A) |
| A' $_{\beta}$ (G) | 80.8/4.52 | ND | C $_{\beta}$ -H $_{\beta}$ in acylated β -O-4 linked to G (A) |
| A $_{\beta}$ (S) | 85.8/4.12 | 79.8/4.63 | C $_{\beta}$ -H $_{\beta}$ in β -O-4 linked to S (A, <i>Erythro</i>) |
| A $_{\beta}$ (S) | 85.8/4.12 | 79.8/4.63 | C $_{\beta}$ -H $_{\beta}$ in β -O-4 linked to S (A, <i>Thero</i>) |
| D $_{\alpha}$ | 81.0/5.10 | ND | C $_{\alpha}$ -H $_{\alpha}$ in spirodienones (D) |
| D' $_{\alpha}$ | 79.4/4.10 | ND | C' $_{\alpha}$ -H' $_{\alpha}$ in spirodienones (D) |
| E $_{\alpha}$ | 79.6/5.60 | ND | C $_{\alpha}$ -H $_{\alpha}$ in α,β -diaryl ethers (E) |
| C $_{\alpha}$ | 86.8/5.45 | 87.1/5.49 | C $_{\alpha}$ -H $_{\alpha}$ in phenylcoumaran (C) |
| T' $_{2,6}$ | 103.9/7.34 | ND | C' $_{2,6}$ -H' $_{2,6}$ in triclin (T) |
| T $_6$ | 98.9/6.23 | ND | C $_{2,6}$ -H $_{2,6}$ in triclin (T) |
| T $_8$ | 94.2/6.60 | ND | C $_8$ -H $_8$ in triclin (T) |
| T $_3$ | 106.2/7.07 | ND | C $_3$ -H $_3$ in triclin (T) |
| S $_{2,6}$ | 103.9/6.70 | 103.5/6.66 | C $_{2,6}$ -H $_{2,6}$ in syringyl units (S) |
| S' $_{2,6}$ | 106.3/7.32 | 105.4/7.37 | C $_{2,6}$ -H $_{2,6}$ in oxidized S units (S') |
| G $_2$ | 110.8/6.97 | 111.0/7.07 | C $_2$ -H $_2$ in guaiacyl units (G) |
| G $_5$ | 114.5/6.70 | 116.5/7.00 | C $_5$ -H $_5$ in guaiacyl units (G) |
| G $_{5e}$ | 115.1/6.95 | ND | C $_5$ -H $_5$ in etherified guaiacyl units (G) |
| G $_6$ | 119.0/6.78 | 118.9/6.90 | C $_6$ -H $_6$ in guaiacyl units (G) |
| J $_{\beta}$ | 126.1/6.76 | ND | C $_{\beta}$ -H $_{\beta}$ in cinnamyl aldehyde end-groups (J) |
| H $_{2,6}$ | 127.7/7.17 | 127.8/7.34 | C $_{2,6}$ -H $_{2,6}$ in H units (H) |
| PCE $_{3,5}$ | 115.6/6.77 | 122.1/7.14 | C $_{3,5}$ -H $_{3,5}$ in <i>p</i> -coumarate (<i>p</i> -CE) |
| PCE $_{2,6}$ | 130.2/7.48 | 129.3/7.68 | C $_{2,6}$ -H $_{2,6}$ in <i>p</i> -coumarate (<i>p</i> -CE) |
| PCE $_7$ | 144.8/7.51 | 143.5/7.52 | C $_7$ -H $_7$ in <i>p</i> -coumarate (<i>p</i> -CE) |
| PCE $_8$ | 113.7/6.24 | 117.4/6.45 | C $_8$ -H $_8$ in <i>p</i> -coumarate (<i>p</i> -CE) |
| FA $_2$ | 110.7/7.35 | ND | C $_2$ -H $_2$ in ferulate (<i>p</i> -FA) |
| FA $_6$ | 123.1/7.20 | ND | C $_6$ -H $_6$ in ferulate (<i>p</i> -FA) |
| FA $_7$ | 144.8/7.51 | 143.5/7.52 | C $_7$ -H $_7$ in ferulate (<i>p</i> -FA) |
| J $_{\alpha}$ | 153.4/7.59 | ND | C $_{\alpha}$ -H $_{\alpha}$ in cinnamyl aldehyde end-groups (J) |

Signal A γ -(δ 63.0/4.36 ppm) appeared in all bamboo lignin samples, indicating that the γ -position of lignin has undergone acylation during the lignification of bamboo, which was consistent with the literature reports [24]. Three basic units of lignin (S, G, H) can be observed in the aromatic ring region and the side chain region (Figure 5). From a structural point of view, the signs of lignin production in one to six year-old bamboo present little changes. The main signals of syringyl unit are A $_{\beta}$ (S)-thero (δ 79.8/4.63 ppm), A $_{\beta}$ (S)-erythro (δ 79.8/4.63 ppm), S $_{2,6}$ (δ 103.5/2.66 ppm), S' $_{2,6}$ (δ 106.3/7.32 ppm). The main signals for the *p*-hydroxytoluene unit are H $_{2,6}$ (δ 127.8/7.34 ppm), H $_{3,5}$ (δ 115.1/6.52 ppm). The main signals of guaiac wood-based units are A $_{\beta}$ (G) (δ 76.6/5.07 ppm), G $_2$ (δ 110.8/6.97 ppm), G $_5$ (δ 114.5/6.71 ppm), G $_6$ (δ 119.0/6.78 ppm). It is proved that the bamboo lignin has three major monomers, which is consistent with the results of FT-IR and ^{13}C NMR.

It is worth noting that there are obvious methoxy signal units (δ 55.6/3.70 ppm) in the side chain region, which is consistent with the ^{13}C NMR result. The main linkage units include β -O-4 ether linkages, β - β , and β -5. The β -O-4 ether bond has three structures: hydroxyl group (A), acetyl group (A'), and esterified pair bean ester (A''). The resin alcohol (B) structural unit also appeared as three signals with α , β , and γ positions at δ 85.1/4.66 ppm, δ 53.7/3.74 ppm, and δ 71.5/4.28 ppm, respectively. All the above connection structure can be detected in 1–6 year-old bamboo lignin, indicating that the connection modes of lignin are similar during the lignification of bamboo.

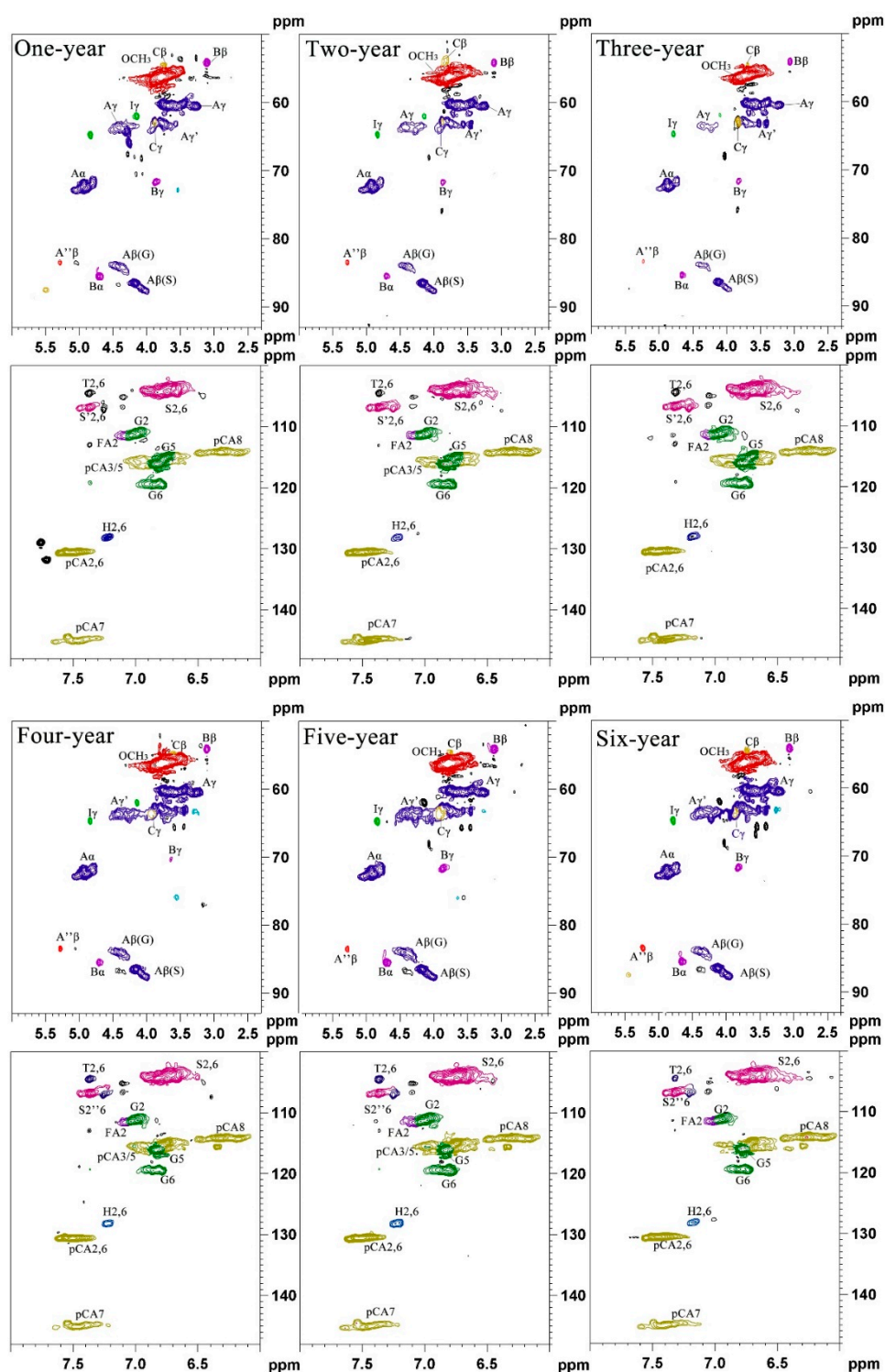


Figure 5. 2D-HSQC NMR spectra of 1–6 year-old bamboo lignins.

3.6. Semiquantitative Estimations Based on 2D-HSQC Spectra

To provide explicit structural evolution of the 1–6 year-old bamboo lignin samples, semiquantitative of the linkages by 2D-HSQC NMR was performed according to the relevant literature [1,8,32]. It is worth noting that G-type lignin is preferentially located in the middle lamella and S-type lignin mainly situated in the inner cell wall area [34]. Different separation methods result in different content of S-type and G-type lignin. In short, ball-milled lignin tends to contain lignin from the middle lamella, whereas

cellulase-digested lignin represents lignin from the secondary cell wall [35]. Therefore, compared to cellulase-digested lignin, the content of G-type lignin in milled bamboo lignin was slightly higher, resulting in a lower S/G ratio. Since the main purpose of this study was to investigate the change of bamboo lignin during lignification process, it was necessary to explore the relative proportion of S/G. As shown in Table 3, S/G ratio has shown an overall upward trend with the bamboo lignification process (1.94–3.02), indicating that the increase rate of S-type lignin content is higher than that of G-type lignin. Therefore, the inner wall area of the cell wall is continuously thickened during the lignification process. This result is consistent with the reported phenomenon by the slice method [19]. Moreover, the deposition of S-type lignin plays an important role in the growth and maturation of angiosperms, which is consistent with the increment of S/G ratio observed in this experiment. The conclusions drawn by the 2D-HSQC semiquantitative method appear to confirm this view. Moreover, the content of β -O-4 ether units shows the similar upward trend (84.13–92.95) as the S/G ratio, which means that S-type lignin content increases constantly. This phenomenon is mainly because the β -O-4 ether unit is mainly connected with S-type lignin [36]. On the other hand, β -O-4 linkage played an important role in angiosperms growth, thus it can act as a pivotal indicator to reflect the lignin complex intactness. The higher the β -O-4 linkage content, the more G-type lignin involved in the construction of β -O-4 dimers [33]. In contrast, the content of resinol substructures and phenylcoumaran show an opposite downward trend. Resinol substructures are the second most abundant interunit in bamboo lignin, which is mainly connecting with G-type lignin by its available 5-position with monolignol β -positions. Thus, the decrease of resinol substructures may be related to the decrease of G-type lignin [35]. The increment of β -O-4 ether unit content is consistent with the GPC results: the Mw of lignin increases with the lignification process. In general, the lower S/G ratio, the more suitable the plant is for the paper-making industry. Lignin will be removed better from bamboo under alkaline conditions with lower S/G ratio, and the fiber strength of the original bamboo will be retained to a greater extent [37]. Therefore, one-year-old bamboo is mainly used in the papermaking industry, while high-grade bamboo is more suitable for the construction field.

Table 3. Quantification of 1–6 year-old bamboo lignin samples by quantitative 2D-HSQC NMR.

| | 1 | 2 | 3 | 4 | 5 | 6 |
|------------------------------|-------|-------|-------|-------|-------|-------|
| S/G ratio | 1.94 | 1.69 | 2.25 | 2.48 | 3.02 | 2.92 |
| β -O-4 ether units (%) | 84.13 | 86.85 | 89.85 | 92.04 | 92.95 | 89.15 |
| Resinol substructures(B) (%) | 4.37 | 4.13 | 2.54 | 1.81 | 1.15 | 2.02 |
| Phenylcoumaran(C) (%) | 1.19 | 1.45 | 0.57 | 0.39 | 0.28 | 0.36 |

4. Conclusions

In this paper, changes in bamboo lignin with age (1–6 years old) were investigated. Results showed that the lignin of 1–6 year-old bamboo contained three monomers of S, G and H with similar chemical structure. The molecular weight of bamboo lignin increases with age. 2D-HSQC NMR semiquantitative results further confirmed that the main change of lignin during the lignification process of bamboo occurs in the monomer content: S/G ratio enhanced with the progress of lignification. The main connecting structure of lignin was the β -O-4 ether bond, and the relative content of β -O-4 ether bond increased during the progress of lignification, which is consistent with the GPC results. Qualitative results showed that the structure of bamboo lignin did not change significantly during the lignification process, while the quantitative results presented that S/G ratio of bamboo lignin increased with age. In the future studies, biological methods such as sectioning and staining observation of cells will be applied to further verify and explore new findings regarding changes of lignin in the bamboo lignification process.

Author Contributions: Formal analysis, Y.Z., J.H., K.W. and S.S.; methodology, B.W., X.L. and L.S.; supervision, L.S., A.W. and H.L.; writing—review and editing, Y.Z., A.W. and H.L. All authors have read and agreed to the published version of the manuscript.

Funding: Financial support for this work was obtained from the National Natural Science Foundation of China (Grant Numbers 31870653, 31811530009, 31700506), the Natural Science Foundation of Zhejiang Province, China (No. LR15C160001), Science and Technology Planning Project of Guangdong Province (No. 2016A010104012), and the Natural Science Foundation of Guangdong Province (No. 2017A030310550).

Conflicts of Interest: The authors declare no conflict of interest.

References

1. Wen, J.L.; Sun, S.L.; Xue, B.L.; Sun, R.C. Structural elucidation of inhomogeneous lignins from bamboo. *Int. J. Biol. Macromol.* **2015**, *77*, 250–259. [[CrossRef](#)] [[PubMed](#)]
2. Obataya, E.; Kitin, P.; Yamauchi, H. Bending characteristics of bamboo (*Phyllostachys pubescens*) with respect to its fiber–foam composite structure. *Wood Sci. Technol.* **2007**, *41*, 385–400. [[CrossRef](#)]
3. Malanit, P.; Barbu, M.; Frühwald, A. Physical and mechanical properties of oriented strand lumber made from an Asian bamboo (*Dendrocalamus asper* Backer). *Eur. J. Wood Wood Prod.* **2011**, *69*, 27–36. [[CrossRef](#)]
4. Maziyar, M.; Housnieh, Y.; Giuseppe, C.; Giuseppe, L.; Calvin, B.; Sui, M.; Atefeh, S.; Pooria, P. Safely dissolvable and healable active packaging films based on alginate and pectin. *Polymers* **2019**, *11*, 1594.
5. Yang, H.; Shi, Z.; Xu, G.; Qin, Y.; Deng, J.; Yang, J. Bioethanol production from bamboo with alkali-catalyzed liquid hot water pretreatment. *Bioresour. Technol.* **2018**, *274*, 261–266. [[CrossRef](#)]
6. Donaldson, L. Microfibril Angle: Measurement, Variation and Relationships—A Review. *IAWA J.* **2008**, *29*, 345–386. [[CrossRef](#)]
7. Wei, P.; Ma, J.; Jiang, Z.; Liu, R.; An, X.; Fei, B. Chemical constituent distribution within multilayered cell walls of moso bamboo fiber tested by confocal raman microscopy. *Wood Fiber Sci.* **2017**, *49*, 12–21.
8. Sun, S.L.; Wen, J.L.; Ma, M.G.; Li, M.F.; Sun, R.C. Revealing the structural inhomogeneity of lignins from sweet sorghum stem by successive alkali extractions. *J. Agric. Food Chem.* **2013**, *61*, 4226–4235. [[CrossRef](#)]
9. Upton, B.; Kasko, A. Strategies for the conversion of lignin to high-value polymeric materials: Review and perspective. *Chem. Rev.* **2015**, *116*, 2275–2306. [[CrossRef](#)] [[PubMed](#)]
10. Zhao, X.H.; Tong, T.; Li, H.; Lu, H.; Ren, J.; Zhang, A.; Deng, X.; Chen, X.; Wu, A. Characterization of hemicelluloses from neolamarckia cadamba (*Rubiaceae*) during xylogenesis. *Carbohydr. Polym.* **2016**, *156*, 333–339. [[CrossRef](#)]
11. Vanholme, R.; De Meester, B.; Ralph, J.; Boerjan, W. Lignin biosynthesis and its integration into metabolism. *Curr. Opin. Biotechnol.* **2019**, *56*, 230–239. [[CrossRef](#)] [[PubMed](#)]
12. Gerpen, J. Biodiesel processing and production. *Fuel Proc. Technol.* **2005**, *86*, 1097–1107. [[CrossRef](#)]
13. Agnieszka, A.; Agnieszka, W.; Krzysztof, P.; Damian, J.; Krzysztof, P.; Marzena, G. The use of lignin as a microbial carrier in the co-digestion of cheese and wafer waste. *Polymers* **2019**, *11*, 2073.
14. Douwe, S.; Coen, A.; Joren, K.; Erwin, W.; Peter, J. Efficient mild organosolv lignin extraction in a flow-through setup yielding lignin with high β -O-4 content. *Polymers* **2019**, *11*, 1913.
15. Wang, B.; Sun, Y.C.; Sun, R.C. Fractional and structural characterization of lignin and its modification as biosorbents for efficient removal of chromium from wastewater: A review. *J. Leather Sci. Eng.* **2019**, *1*, 5–30. [[CrossRef](#)]
16. Lan, W.; Lu, F.; Regner, M.; Zhu, Y.; Rencoret, J.; Ralph, S.; Zakai, U.; Morreel, K.; Boerjan, W.; Ralph, J. Tricin, a flavonoid monomer in monocot lignification. *Plant Physiol.* **2015**, *167*. [[CrossRef](#)]
17. Li, C.; Xuan, L.; He, Y.; Wang, J.; Zhang, H.; Ying, Y.; Wu, A.; Bacic, A.; Zeng, W.; Song, L. Molecular mechanism of xylogenesis in moso bamboo (*Phyllostachys edulis*) shoots during Cold Storage. *Polymers* **2018**, *11*, 38. [[CrossRef](#)]
18. Lybeer, B.; Koch, G.; Van Acker, J.; Goetghebeur, P. Lignification and cell wall thickening in nodes of *Phyllostachys viridiglaucescens* and *Phyllostachys nigra*. *Ann. Bot.* **2006**, *97*, 529–539. [[CrossRef](#)]
19. Sluiter, J.; Ruiz, R.; Scarlata, C.; Sluiter, A.; Templeton, D. Compositional analysis of lignocellulosic feedstocks. 1. Review and description of methods. *J. Agric. Food Chem.* **2010**, *58*, 9043–9053. [[CrossRef](#)]
20. Wen, J.L.; Sun, S.L.; Xue, B.L.; Sun, R.C. Quantitative structural characterization of the lignins from the stem and pith of bamboo (*Phyllostachys pubescens*). *Holzforschung* **2013**, *67*, 613–627. [[CrossRef](#)]
21. Wen, J.L.; Xue, B.L.; Xu, F.; Sun, R.C. Unveiling the structural heterogeneity of bamboo lignin by in situ HSQC NMR technique. *BioEnergy Res.* **2012**, *5*, 886–903. [[CrossRef](#)]

22. Wang, K.; Wang, B.; Hu, R.; Zhao, X.; Li, H.; Zhou, G.; Song, L.; Wu, A. Characterization of hemicelluloses in *Phyllostachys edulis* (Moso bamboo) culm during xylogenesis. *Carbohydr. Polym.* **2019**, *221*, 127–136. [[CrossRef](#)]
23. He, J.B.; Zhao, X.H.; Du, P.Z.; Zeng, W.; Beahan, C.; Wang, Y.Q.; Li, H.L.; Bacic, A.; Wu, A. KNAT7 positively regulates xylan biosynthesis by directly activating IRX9 expression in Arabidopsis: KNAT7 positively regulates xylan biosynthesis. *J. Integr. Plant Biol.* **2018**, *60*, 514–528. [[CrossRef](#)] [[PubMed](#)]
24. Yen, T.M. Culm height development, biomass accumulation and carbon storage in an initial growth stage for a fast-growing moso bamboo (*Phyllostachy pubescens*). *Bot. Stud.* **2016**, *57*, 10–19. [[CrossRef](#)] [[PubMed](#)]
25. Liese, W.; Weiner, G. Ageing of bamboo culms. A review. *Wood Sci. Technol.* **1996**, *30*, 77–89. [[CrossRef](#)]
26. Faix, O. Classification of lignins from different botanical origins by FT-IR spectroscopy. *Holzforschung* **1991**, *45*, 21–28. [[CrossRef](#)]
27. Li, M.F.; Sun, S.N.; Xu, F.; Sun, R.C. Formic acid based organosolv pulping of bamboo (*Phyllostachys acuta*): Comparative characterization of the dissolved lignins with milled wood lignin. *Chem. Eng. J.* **2012**, *179*, 80–89. [[CrossRef](#)]
28. Abdelkafi, F.; Houcine, A.; Rousseau, B.; Tessier, M.; Gharbi, R.; Fradet, A. Structural analysis of alfa grass (*Stipa tenacissima* L.) lignin obtained by acetic acid/formic acid delignification. *Biomacromolecules* **2011**, *12*, 3895–3902. [[CrossRef](#)]
29. Gluseppe, C.; Aurelio, A.; Lorenzo, L. Comparative study of historical woods from XIX century by thermogravimetry coupled with FTIR spectroscopy. *Cellulose* **2019**, *26*, 8853–8865.
30. Kai, D.; Tan, M.; Chee, P.L.; Chua, Y.; Yap, Y.; Loh, X.J. Towards lignin-based functional materials in a sustainable world. *Green Chem.* **2016**, *18*, 1175–1200. [[CrossRef](#)]
31. Guerra, A.; Mendonça, R.; Ferraz, A.; Lu, F.; Ralph, J. Structural characterization of lignin during pinus taeda wood treatment with ceriporiopsis subvermispora. *Appl. Environ. Microb.* **2004**, *70*, 4073–4078. [[CrossRef](#)] [[PubMed](#)]
32. Wen, J.L.; Xue, B.L.; Xu, F.; Sun, R.C.; Pinkert, A. Unmasking the structural features and property of lignin from bamboo. *Ind. Crop. Prod.* **2013**, *42*, 332–343. [[CrossRef](#)]
33. Li, M.F.; Fan, Y.M.; Xu, F.; Sun, R.C. Characterization of extracted lignin of bamboo (*Neosinocalamus affinis*) pretreated with sodium Hydroxide/urea solution at low temperature. *Bioresources* **2010**, *5*, 1762–1778.
34. Zhou, C.; Li, Q.; Chiang, V.; Lucia, L.; Griffis, D. Chemical and spatial differentiation of syringyl and guaiacyl lignins in poplar wood via Time-of-Flight secondary ion mass spectrometry. *Anal. Chem.* **2011**, *83*, 7020–7026. [[CrossRef](#)] [[PubMed](#)]
35. Zeng, J.; Helms, G.; Gao, X.; Shulin, C. Quantification of wheat straw lignin structure by comprehensive NMR analysis. *J. Agric. Food Chem.* **2013**, *61*, 4226–4235. [[CrossRef](#)]
36. Sun, X.-F.; Sun, R.; Fowler, P.; Baird, M. Extraction and characterization of original lignin and hemicelluloses from wheat straw. *J. Agric. Food Chem.* **2005**, *53*, 860–870. [[CrossRef](#)]
37. Xiao, L.P.; Xu, F.; Sun, R.C. Chemical and structural characterization of lignins isolated from *Caragana sinica*. *Fibers Polym.* **2011**, *12*, 316–323. [[CrossRef](#)]

